JCB Article

A novel role for dp115 in the organization of tER sites in *Drosophila*

Vangelis Kondylis[1,2] and Catherine Rabouille[1,2]

[1]The Wellcome Trust Centre for Cell Biology, Institute for Cell and Molecular Biology, University of Edinburgh, Edinburgh, UK
[2]Department of Cell Biology, University Medical Centre Utrecht, Academic Ziekenhuis Utrecht, 3584CX Utrecht, Netherlands

Here, we describe that depletion of the *Drosophila* homologue of p115 (dp115) by RNA interference in *Drosophila* S2 cells led to important morphological changes in the Golgi stack morphology and the transitional ER (tER) organization. Using conventional and immunoelectron microscopy and confocal immunofluorescence microscopy, we show that Golgi stacks were converted into clusters of vesicles and tubules, and that the tERs (marked by Sec23p) lost their focused organization and were now dispersed throughout the cytoplasm. However, we found that this morphologically altered exocytic pathway was nevertheless largely competent in anterograde protein transport using two different assays. The effects were specific for dp115. Depletion of the *Drosophila* homologues of GM130 and syntaxin 5 (dSed5p) did not lead to an effect on the tER organization, though the Golgi stacks were greatly vesiculated in the cells depleted of dSed5p. Taken together, these studies suggest that dp115 could be implicated in the architecture of both the Golgi stacks and the tER sites.

Introduction

The Golgi apparatus exhibits a unique membrane architecture comprising Golgi stacked cisternae. There is accumulating evidence, particularly from yeast studies, suggesting a relationship between the presence of the Golgi stacks and a focused organization of the transitional ER (tER)* sites (Glick, 2002). tER sites are defined as specialized ER subdomains at which proteins destined for the Golgi apparatus are packaged into transport vesicles. They are defined by the presence of COPII vesicles, which carry the secretory cargo out of the ER. Cells contain many tER sites, where the COPII components Sec23p, Sec13p, and Sar1p have been localized (Orci et al., 1991; Barlowe et al., 1994). tER sites often display an elaborate architecture of clustered pleiomorphic membranes comprising one cup-shaped ER cisternae where budding profiles can be observed, small 50–70-nm vesicles (sometimes coated), and short tubules (Bannykh et al., 1996). However, the molecular mechanism that generates them is still mysterious (Rossanese et al., 1999).

In yeast *Pichia pastoris*, the Golgi apparatus exhibits stacked cisternae with established polarity, and the pattern of Sec13–GFP representing the tERs comprised two to six spots surrounding the nucleus. In contrast, *Saccharomyces cerevisiae* exhibits a Golgi apparatus in a form of multiple single cisternal elements surrounded by vesicles and tubules, which represent either the cis or the trans side of the Golgi (Preuss et al., 1992). Sec13–GFP appears in multiple fluorescent dots, indicating that the tER sites are dispersed throughout the ER. The reasoning sustaining the relationship between the tER organization and the presence of polarized Golgi stacks is that the concentration of vesicles budding from focused tER sites would remain high enough, maybe due to the presence of a tER matrix, to allow cisternal formation and stacking (Rossanese et al., 1999; Bevis et al., 2002), whereas the membrane derived from dispersed tERs is too low in concentration for proper cisternal formation and further stacking. However, the nature of the tER matrix is far from being clear.

On the other hand, studies performed in mammalian cells have established a number of so-called "Golgi matrix proteins," most of them Golgins such as p115, GM130, and giantin, that are involved in the building and maintenance of the Golgi stacks (Shorter and Warren, 2002). These proteins were characterized by the fact that they are not relocated to the ER upon brefeldin A treatment (Seemann et al., 2000a). These proteins have been shown and/or postulated to help

The online version of this article includes supplemental material.

Address correspondence to Catherine Rabouille, Department of Cell Biology, University Medical Centre Utrecht, AZU Room G02.525, Heidelberglaan 100, 3584CX Utrecht, Netherlands. Tel.: 31-30-250 9280. Fax: 31-30-254 1797. E-mail: C.Rabouille@lab.azu.nl

*Abbreviations used in this paper: GA, glutaraldehyde; IEM, immunoelectron microscopy; RNAi, RNA interference; tER, transitional ER.

Key words: *Drosophila* S2 cells; Golgi apparatus; tER sites; RNAi; p115

the Golgi stacks adopt this typical architecture of stacked cisternae (see Discussion).

Golgi matrix proteins have been localized in mammalian cells to the Golgi area but also in earlier secretory compartments, rather away from the Golgi complex. p115, for instance, has been localized in the intermediate compartment and has been involved in ER to Golgi transport (Nelson et al., 1998; Alvarez et al., 1999, 2001). p115 has also been shown to be recruited on COPII vesicles by Rab1 and prime them for fusion with the Golgi membranes by recruiting a SNARE protein complex (Allan et al., 2000). Finally, Uso1p, the yeast functional orthologue of p115, has been implicated in early transport events such as ER-derived vesicle tethering and proper protein sorting (Sapperstein et al., 1995; Morsomme and Riezman, 2002), indicating that it could be localized in this part of the exocytic pathway. This opens the possibility that, in addition to its role in the different transport steps, p115 could also have a role in the organization of the tER sites.

In fly, the organization of the exocytic pathway is slightly different from the mammalian one. Golgi stacks are not interconnected to form a single copy organelle capping the nucleus. Instead, they remain dispersed in the cytoplasm (Rabouille et al., 1999), as is the case in plants and *Pichia*. The simplified organization observed in *Drosophila* provides us with the possibility to examine the molecular mechanisms underlying both structures in relation to each other. This could allow us to investigate whether the architecture of the Golgi apparatus in *Drosophila* S2 cells is a direct consequence of the tER organization or whether their structural organization is regulated independently of each other.

In the present study, we show that depletion of the *Drosophila* homologue of p115, dp115, which is localized both in the Golgi stacks and in dSec23p-positive tERs, led to a quantitative breakdown of Golgi stacks that are converted into Golgi clusters of vesicles and tubules and strongly affected the general organization of the tER sites. In addition, we show that despite the presence of a morphologically modified exocytic pathway, the intracellular transport was largely unaffected, suggesting that the disorganized tER and the Golgi clusters still form a functional exocytic pathway.

Results

The localization of dp115 in *Drosophila* S2 cells

Drosophila p115 (dp115) exhibits 60% similarity to its rat counterpart (Fig. 1 A). dp115 does not possess the acidic stretch of the 50 COOH-terminal amino acids that has been shown in rat p115 to be involved in binding GM130 and giantin (Dirac-Svejstrup et al., 2000). In dp115, there are only a few acidic amino acids scattered along the last 100 COOH-terminal portion of the protein. Besides *Neurospora*, the tail of *Caenorhabditis elegans* and *Arabidopsis* p115 homologues is not acidic either, except for the last 5 and 15 amino acids, respectively (our search). However, the domain in GM130 that binds p115 is conserved in dGM130 (Kondylis et al., 2001; Fig. 1 A), suggesting that both *Drosophila* proteins could bind each other (albeit possibly through a different domain in dp115).

Despite the high level of homology between mammalian and *Drosophila* p115, we were interested to verify the localization of the *Drosophila* homologue. dp115 has been shown to localize to the Golgi apparatus and Golgi clusters in *Drosophila* imaginal discs by an antibody raised against rat p115 that cross reacted with dp115 (Kondylis et al., 2001). We raised an antibody against a dp115-specific peptide (dp115/584) that recognizes three bands by Western blotting (Fig. 1 B), one at 40 kD (resulting from the secondary antibody, because it is present in the absence of primary antibody; unpublished data), one at 65 kD, and one at 85 kD (Fig. 1 B, lane 1), which has the predicted molecular mass for dp115. We fractionated the S2 cell extract into cytosolic and membrane fractions. After blotting, the 85-kD band seemed only associated with the membrane fraction (lane 3), although its absence from the cytoplasmic fraction (lane 2) might be due to insufficient loading. In larval extract, this band was the major one, and the 65-kD band was much weaker (lane 5). The 65-kD band was considered nonspecific because Western blotting of embryo extracts did not show any bands at 85-kD but revealed a 65-kD band with the same intensity as the larval extract (lane 4). Furthermore, the intensity of this band did not vary according to the amount of protein loaded (unpublished data), and it was present in other Western blots using different primary antibodies.

When used in immunoelectron microscopy (IEM), the dp115/584 antibody gave a specific signal (Fig. 1, C–F). In S2 cells, 30 ± 5% of the gold particles were on the cytoplasm. The Golgi area was labeled by 25 ± 8% of the membrane-associated gold particles. The ER cisternae were decorated by 21 ± 6%. Pleiomorphic membranes (Fig. 1, C and D, asterisk) comprising tubules and vesicles (50–70 nm in diameter, but also larger vessels) close to the Golgi stacks or in their neighborhood contained 54 ± 7% of the membrane-associated labeling. A double labeling with an antibody recognizing the *Drosophila* homologue of Sec23p (dSec23p; Fig. 1, E and F) suggested that these pleiomorphic membranes represented tERs (see Fig. 5). The linear density of gold particles over the membrane of these three compartments was estimated to be 0.57 gold/μm on the Golgi membrane, 0.37 on tER membrane, and 0.15 on ER cisternae. A similar pattern of distribution was observed when salivary glands of third instar larvae were labeled with the same antibody (Fig. 1 D).

dGM130 has been described in Kondylis et al. (2001) and localizes to the Golgi apparatus in *Drosophila* imaginal discs. When MLO7 (a polyclonal antibody directed against the first 73 amino acids of GM130; a gift from Martin Lowe, University of Manchester, Manchester, UK) was used in S2 cells for indirect immunofluorescence, it labeled dGM130 in a Golgi-specific manner (unpublished data).

Effect of depleting dp115 and dGM130 on Golgi stack morphology

We depleted S2 cells of dGM130 using a dsRNA corresponding to the second exon of dGM130 (ds dGM130). When samples were analyzed by Western blotting, two bands were detected, one very faint, which was neglected (Fig. 2, top, lane C), and a strong one. The strong band

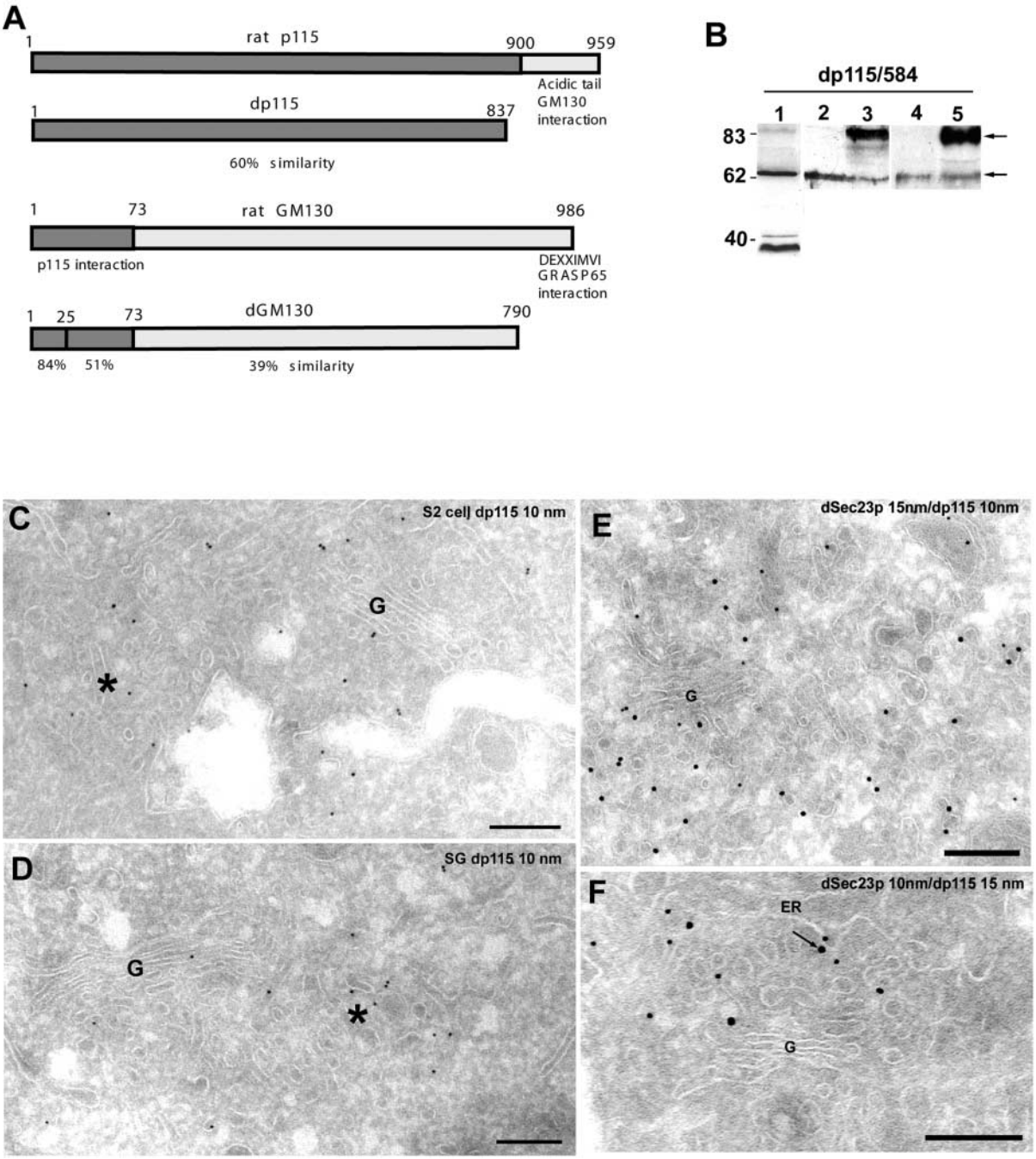

Figure 1. **dp115 in *Drosophila* S2 cells.** (A) dGM130 and dp115 proteins were compared with their rat homologues, and the domains of highest homology are painted in dark gray. (B) Western blotting using the affinity-purified dp115/584 of total S2 cell extract corresponding to 2,000,000 cells (lane 1), 4% of the cytosolic fraction of 10,000,000 cells (lane 2), the total membrane corresponding to 10,000,000 cells (lane 3), total extract corresponding to 20 embryos (lane 4), one third instar larva (lane 5). Two bands were recognized (small arrows on the right). Molecular mass markers are indicated on the left. (C–F) IEM of dp115 on *Drosophila* cells and tissues. Cryosections of PFA (C and E) and PFA/GA (F) fixed S2 cells and *Drosophila* third instar larvae salivary glands (D) were incubated with the affinity-purified dp115/584 and 10-nm protein A gold. (E) S2 cell sections were double labeled with the dp115/584 antibody followed by 10-nm protein A gold, and the Sec23p antibody followed by 15-nm protein A gold. (F) The same labeling was performed but the gold sizes are inverted. Golgi stacks are marked by a G, and pleiomorphic membranes are marked by an asterisk in C and D. The arrow indicates dp115 in an ER bud in F. Bars, 200 nm.

migrated at the predicted position for a protein of the mass of dGM130 (arrow) and was reduced below detectable level after 48 h (Fig. 2, top) and remained so up to 120 h of incubation. This depletion, however, did not lead to any effect on Golgi stack morphology, as assessed by EM (Fig. 3 B).

The percentage of cell sections exhibiting at least one Golgi stack per cell profile was scored. 100% of mock-treated (incubated without dsRNA) and mock-depleted cells (incubated with ds EGFP) exhibited at least one Golgi stack per cell profile (Fig. 3 A). This percentage decreased slightly to 85% for incubations up to 96 and 120 h. On average,

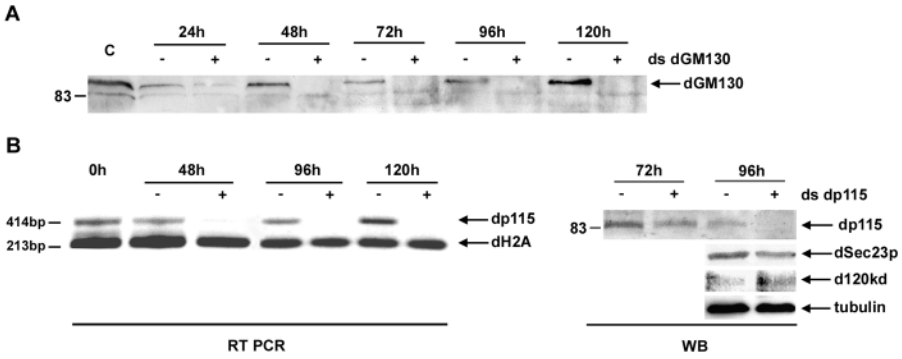

Figure 2. **Depletion of dGM130 protein and dp115 mRNA.** (A) Western blotting using MLO7 (anti-GM130 antibody) of the extract of S2 cells incubated with (+) or without (−) ds dGM130 for increasing lengths of time. C corresponds to time 0 (3,000,000 cells). 1,500,000 cells were used for lanes 24–72 h, and 2,500,000 for lanes 96–120 h. From the two bands the antibody recognizes, the stronger upper band is specifically depleted (arrow). (B) The dp115 mRNA was measured by RT-PCR from total RNA extract from 1,000,000 cells incubated with (+) or without (−) ds dp115 for 48–120 h. Amplification of histone 2A mRNA was used as control of the specific depletion of dp115 mRNA and as a loading control. Western blotting of the extract of cells (1,500,000) incubated with (+) or without (−) ds dp115 for 72 and 96 h using the dp115/584 antibody (dp115), the Sec23p antibody (dSec23p), the antibody recognizing the 120-kD *Drosophila* antigen (d120kd), and α-tubulin. Note that only dp115 is depleted.

these Golgi stacks had a cross-sectional diameter of 0.368 ± 0.047 μm and 3.7 ± 0.8 cisternae per stack.

In cells depleted of dGM130, the percentage of cells exhibiting Golgi stacks (Fig. 4 A), the number of cisternae per stack, and the mean diameter of the stacks were comparable to the figures obtained for mock-treated cells (diameter of 0.347 ± 0.078 μm and 3.5 ± 1.6 cisternae per stack).

We depleted S2 cells of dp115. dsRNA corresponding to the NH_2-terminal portion of dp115 (ds dp115) was added to S2 cells for up to 120 h. We first assessed the depletion of dp115 mRNA by RT-PCR using primers corresponding to the 5′ end of the dp115 gene (Fig. 2 B, RT PCR). After 48 h, dp115 mRNA could not be detected and remained so up to 120 h. Western blotting with the dp115/584 antibody showed that the 85-kD band disappeared after 96 h of incubation with ds dp115 (Fig. 2 B, WB).

Cells depleted of dp115 up to 72 h did not show significant changes in their Golgi stack morphology when compared with controls (Fig. 3 C). 76.3 ± 4.0% exhibited at least one Golgi stack per cell section (Fig. 4 A). However, this percentage decreased sharply in the cells incubated for 96 h. In only 18 ± 6.3% of the cell sections, one or more

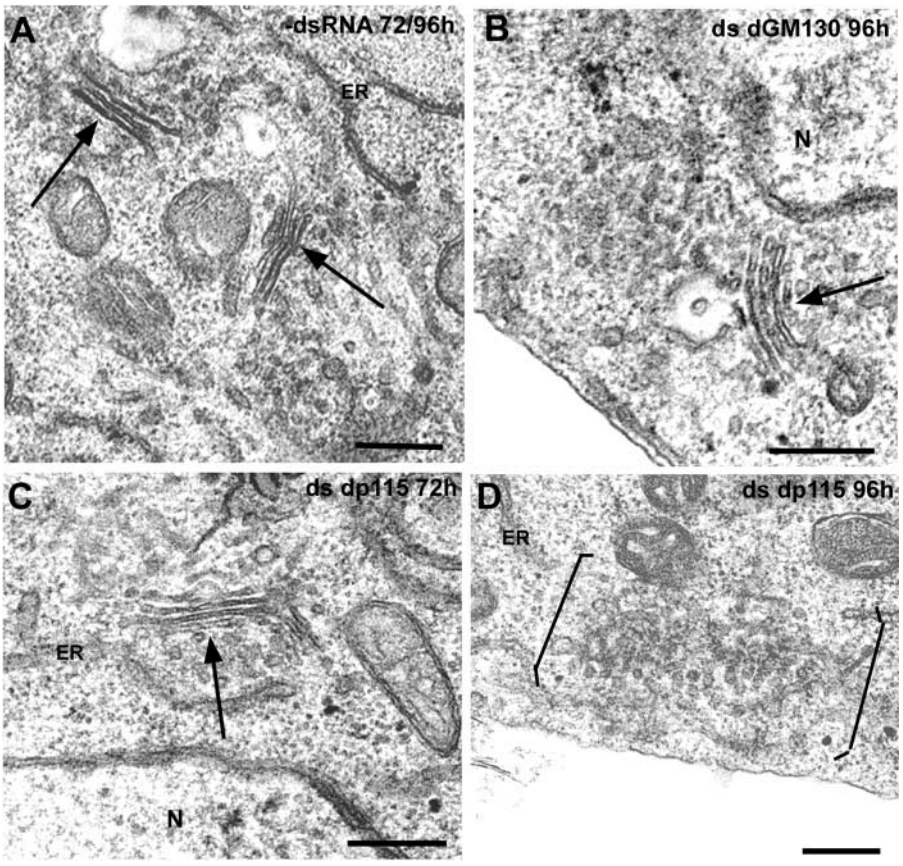

Figure 3. **Effect of depleting dp115 and dGM130 on the Golgi stack morphology.** *Drosophila* S2 cells were cultured (A) in the absence (−dsRNA) or (B) presence of ds dGM130 for 96 h, or (C) in the presence of ds dp115 for 72 or (D) 96 h. Cells were collected and processed for conventional EM. Golgi stacks are indicated with a long arrow, and clusters of vesicles and tubules are marked between brackets. N, nucleus. Bars, 200 nm.

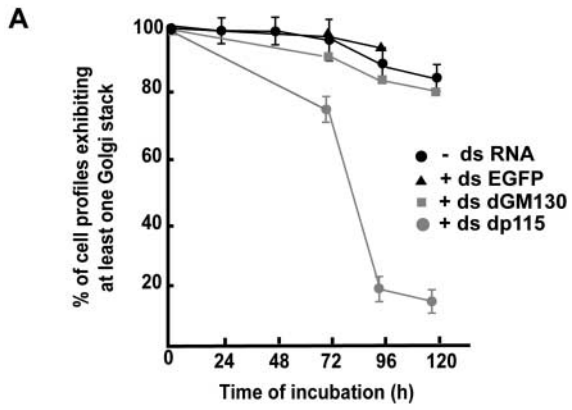

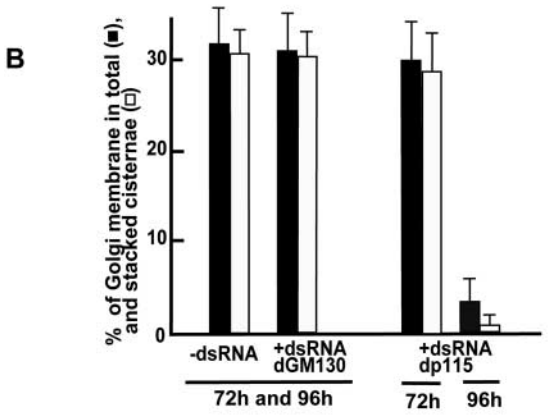

C

Estimation of the surface density of the Golgi area (SDgo) and the total cisternae (SDcis).

	Mock depleted 96h	dp115 depleted 96h
SD go	3.64 ± 0.44	2.97±0.29
SD cis	1.25±0.17	0.16±0.07

Figure 4. **Quantitative analysis of the morphological effects after protein depletion.** (A) Percentage of Golgi stacks in profiles of S2 cells depleted of dp115 and dGM130. S2 cells were incubated for 24 to 120 h with the different dsRNAs, processed for EM, and scored for the presence of at least one Golgi stack per cell profile. The results obtained are presented as a percentage of the total number of cells examined for each condition (~300). (B) Stereological analysis of the Golgi area after protein depletion. Representative EM pictures of mock-treated cells and cells depleted of dGM130 and dp115 at 72 and 96 h were used to estimate the percentage of Golgi membrane in total cisternae (black bars) and stacked cisternae (white bars). The error bars represent the SD. (C) Estimation of the surface density of the Golgi area (SDgo) and the total cisternae (stacked and single) (SDcis) in mock- and dp115-depleted cells for 96 h. Results are expressed in μm^{-1} and ± represents SD.

Golgi stacks were visible (Fig. 4 A). These stacks were also smaller than in mock-depleted cells with a mean diameter of 0.268 ± 0.050 μm and 3.2 ± 0.4 cisternae/stack. The remaining 82% of the cell sections exhibited a Golgi area under the form of clusters of vesicles and tubules (Fig. 3 D). The percentage of membrane in cisternae per Golgi area decreased by 12% at 72 h, and by 87% at 96 h, when compared with control (Fig. 4 B). This latter decrease was paralleled by a decrease in stacking (Fig. 4 B) and was mirrored by an increase of 32% in vesicular profiles and an increase of 50% of small tubules.

The surface density of the Golgi area (SDgo) and total cisternae (SDcis) (stacked and single) was estimated in mock- and dp115-depleted cells. A reduction of 21% of SDgo was observed after dp115 depletion together with a reduction of 88% of the SDcis (Fig. 4 C), suggesting that cisternal profiles were lost or not merely diluted, for instance, by incoming vesicles that would accumulate around them, unable to fuse due to lack of dp115.

Effect of dp115 depletion on the tER organization

Given the impact of dp115 depletion on the structure of the Golgi stacks, the proposed relationship between the tER organization and the presence of Golgi stacks, and the presence of dp115 at the tERs, we were prompted to look at the organization of the tER sites in cells depleted of dp115.

For this purpose, two antibodies were used. First, a polyclonal antibody raised against a rat Sec23p peptide (conserved in *Drosophila*) was used for IEM on S2 cell cryosections. This antibody decorated pleiomorphic membrane populated with 50–70-nm vesicular profiles (some coated; Fig. 5, D and E), ER coated buds, as well as larger vesicular and tubular membrane structures, often contained in the concavity of an ER cisterna (Fig. 5, A and C–E). These structures are reminiscent of those described by Bannykh et al. (1996), referred to as vesicular tubular clusters (VTCs). Since then, the VTC terminology has been used to describe other structures in the intermediate compartment. To avoid a possible misunderstanding, we refer to our membrane structures as tER sites on the basis of their dSec23p labeling and their colocalization with a transport cargo, such as the plasma membrane protein Delta (Fig. 5 F; see below). The gold labeling density on the tER sites was six to seven times higher than in the surrounded cytoplasm. Furthermore, 10 ± 3% of the gold particles decorated the ER cisternae.

Second, a monoclonal antibody recognizing a 120-kD *Drosophila* Golgi membrane antigen (d120kd; Stanley et al., 1997) was tested by IEM. The gold labeling was specific to the Golgi apparatus. 55% labeled the Golgi stacks, and 35% labeled vesicles and tubules abutting the Golgi stack (Fig. 5, B and C), a result in agreement with immunofluorescence data (Stanley et al., 1997; Munro and Freeman, 2000).

In immunofluorescence, these two antibodies gave similar patterns. The dSec23p pattern corresponded to 20 ± 8 large fluorescent objects dispersed in the cytoplasm (Fig. 6 A). The d120kd pattern corresponded to 18 ± 7 similar large fluorescent objects (Fig. 6 B). These two patterns overlapped partially (Fig. 6 C). By IEM, the region of overlap corresponded to the interface between the Golgi stack and the tER where the two antigens are in close proximity (Fig. 5 C).

In cells depleted of dp115 for 96 h, however, both patterns were differentially affected. In 90% of the cells, the immunofluorescence pattern of dSec23p appeared as numerous scattered small dots all over the cytoplasm (84.5 ± 20/cell; Fig. 6 D). The size of these fluorescent objects was approxi-

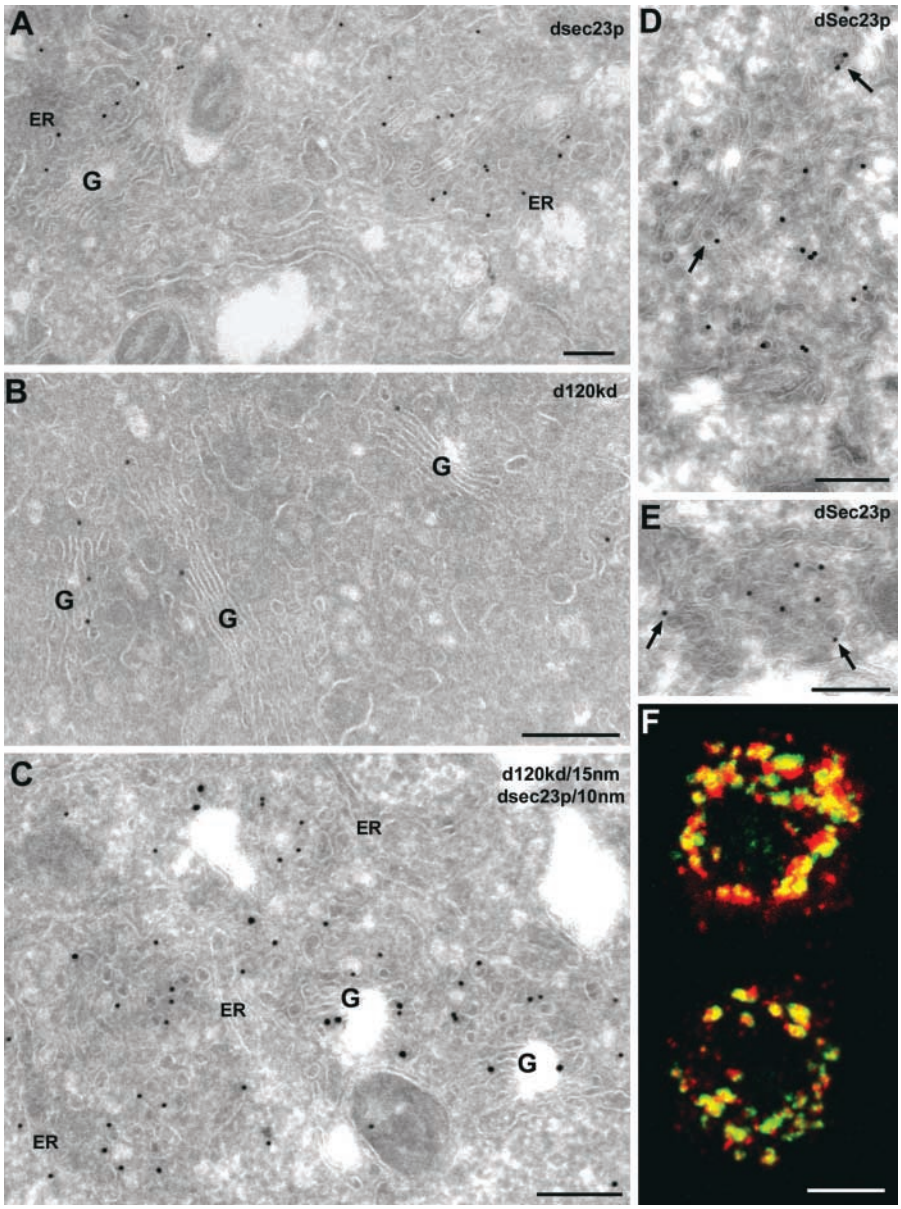

Figure 5. **Localization of d120kd and dSec23p in S2 cells.** Cryosections of *Drosophila* S2 cells, fixed with PFA/GA (A–C) or PFA alone (D and E), were labeled (A, D, and E) with a polyclonal anti-Sec23p antibody (10-nm gold) or (B) a monoclonal antibody against d120kd (10-nm gold). (C) Sections were double labeled with the d120kd antibody (15-nm gold) and the anti-Sec23p antibody (10-nm gold). (F) Delta S2 cells were induced with CuSO4 for 25 min and processed for immunofluorescence. Delta and dSec23p were labeled using C594.9B (red) and the anti-Sec23p antibody (green), respectively. The merge projections of 30 confocal sections are presented, and the overlap is yellow. The COPII coats labeled for dSec23p are indicated with an arrow. G, Golgi stacks. Bars: (A–E) 200 nm; (F) 5 μm.

mately three to four times smaller when compared with mock-depleted cells. The d120kd pattern of fluorescence also changed after dp115 depletion (Fig. 6 E). The number of fluorescent objects corresponding to this antigen was slightly higher than in control cells (26 ± 7 vs. 18 ± 6 in control cells), but their size was smaller, and the intensity of fluorescence reduced, as if this antigen was dispersed. d120kd and dSec23p immunofluorescence patterns did not overlap as much as in mock-treated cells. Numerous dSec23p dots seemed to be free of d120kd, and ~50% of the d120kd-positive dots were also observed free of dSec23p (Fig. 6 F). Similar changes in patterns were also observed when the cells were fixed with stronger fixatives and for a longer period of time, suggesting that the observed effects were not due to mild fixation (see Fig. S1, available at http://www.jcb.org/cgi/content/full/jcb.200301136/DC1). Furthermore, dSec23p and d120kd were not degraded upon dp115 depletion (Fig. 2 B), suggesting that this was not the cause of the change in patterns.

In dp115-depleted cells observed by IEM, the dSec23p-positive small and scattered dots observed in immunofluorescence represented pleiomorphic membranes containing vesicles and tubules, reminiscent of those observed in control cells, but with a smaller size (compare Fig. 5 A with Fig. 7, A and B; see Fig. S2, A and B, available at http://www.jcb.org/cgi/content/full/jcb.200301136/DC1). They appeared more dispersed throughout the cytoplasm than in control cells and sometimes exhibited a reduced labeling density (Fig. 7, B and E). The number of these dSec23p-positive sites per cell section was 6.7 ± 2.3, and only 20% of them were positive for d120kd. This is to be compared with 2.7 ± 1.5 dSec23p-positive sites per section of mock-depleted cells, 90% of them also positive for d120kd (Fig. 5 C), suggesting that small tER sites have been generated that lack the spatial relationship with Golgi areas.

The d120kd-positive dots that were observed in immunofluorescence represented clusters of vesicles and tubules labeled by 73 ± 3.6% of the gold particles associated with

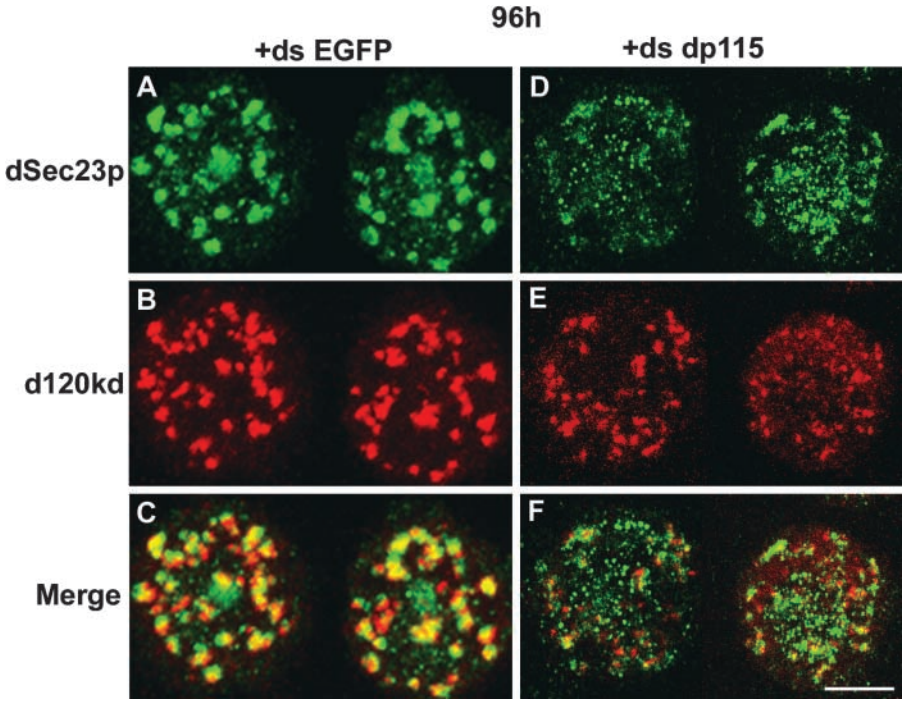

Figure 6. **Effect of dp115 depletion on the organization of the tER sites.** S2 cells were processed for confocal immunofluorescence microscopy using the anti-Sec23p antibody (green; A and D) and the d120kd antibody (red; B and E) in mock-depleted (+ds EGFP; A–C) and dp115-depleted cells (+ds dp115; D–F). Projections of 30 sections are presented, and in merge images (C and F), the overlap is yellow. Note that in mock-depleted cells, almost every dSec23p-positive structure is found in close proximity to a d120kd-positive one. Bar, 5 μm.

d120kd (Fig. 7, C–F). In these clusters, we could observe profiles reminiscent of short cisternal remnants (Fig. 7, D–F, arrows), indicating that these clusters could derive from Golgi stack breakdown. d120kd also labeled the ER cisternae (27 ± 3.6%; Fig. 7 E, arrowhead), suggesting perhaps a retrograde movement of Golgi membrane to the ER.

Pleiomorphic membranes of vesicles and tubules were also labeled by both dSec23p and d120kd, showing that some tERs have remained in close proximity to the Golgi membrane, as they were in nondepleted cells. In some cases, these two markers did not label the pleiomorphic membrane homogeneously and seemed to retain their original polarity (Fig. 7, D–F).

Overall, this experiment shows that the depletion of dp115 leads to the disorganization of both the tER sites and the Golgi stacks, suggesting that dp115 could be involved in the organization of both. Alternatively, the disorganization of the tERs could lead to the destabilization on the Golgi stacks. dp115 could thus have only one role in tER organization. To test this hypothesis, we assessed the immunofluorescence pattern of dSec23p and d120kd in dp115-depleted S2 cells between 72 and 96 h after ds dp115 addition (see Fig. S3, available at http://www.jcb.org/cgi/content/full/jcb.200301136/DC1). After a 72-h incubation with ds dp115, both dSec23p and d120kd patterns were almost indistinguishable from mock-treated cells (~20 large fluorescent objects partially overlapping, which we will refer to as "control patterns"). However, after 84, 88, and 92 h incubation, a mixture of patterns was observed. The number of cells exhibiting control patterns decreased gradually over time to reach 12.6% after 96 h incubation. Conversely, the cells exhibiting a pattern where both dSec23p and d120kd were affected increased gradually from 17.6 to 83.8%. The percentage of cells where only the dSec23p pattern was affected was roughly the same (2.3%) as that of cells where only the d120kd pattern was affected (0.9%). This result suggests that depletion of dp115 leads to a concomitant loss of Golgi stacks and tER organization, indicating that dp115 could have a distinct role in the organization of both structures.

These effects were specific for dp115 depletion. dGM130 depletion did not have any effect either on the structure of the Golgi complex (Fig. 3 B) or on tER organization (Fig. 8 E). On the other hand, depletion of dSed5p, the *Drosophila* homologue of mammalian syntaxin 5 (Banfield et al., 1994), had a very strong effect on the Golgi stack morphology (complete and quantitative vesiculation; Fig. 8, A and B), but the organization of the tERs was kept intact (Fig. 8 D) when compared with mock-depleted cells (Fig. 8 C). The fragmentation of the Golgi stacks therefore did not cause the redistribution of the tER sites.

Effect of the depletion of dp115 and dGM130 on anterograde protein transport

Depletion of dp115 led to quantitative breakdown of the Golgi stacks and dispersal of the tER sites. That prompted us to test whether this morphologically modified exocytic pathway was still functional.

We used an S2 cell line stably transfected with a construct expressing the full-length plasma membrane protein Delta (Klueg et al., 1998), referred to as Delta S2 cells. Delta is a glycosylated *Drosophila* ligand of Notch (Panin et al., 2002) that uses the exocytic pathway for its plasma membrane deposition (Fig. 5 F; see Fig. S4, available at http://www.jcb.org/cgi/content/full/jcb.200301136/DC1). The expression of Delta in this cell line is under the control of a metallothionein promoter, and addition of $CuSO_4$ drives its expression. The morphological effects of the various depletions were strictly similar in Delta S2 cells and in wild-type S2 cells, and all our stereological analyses have been obtained with both cell lines.

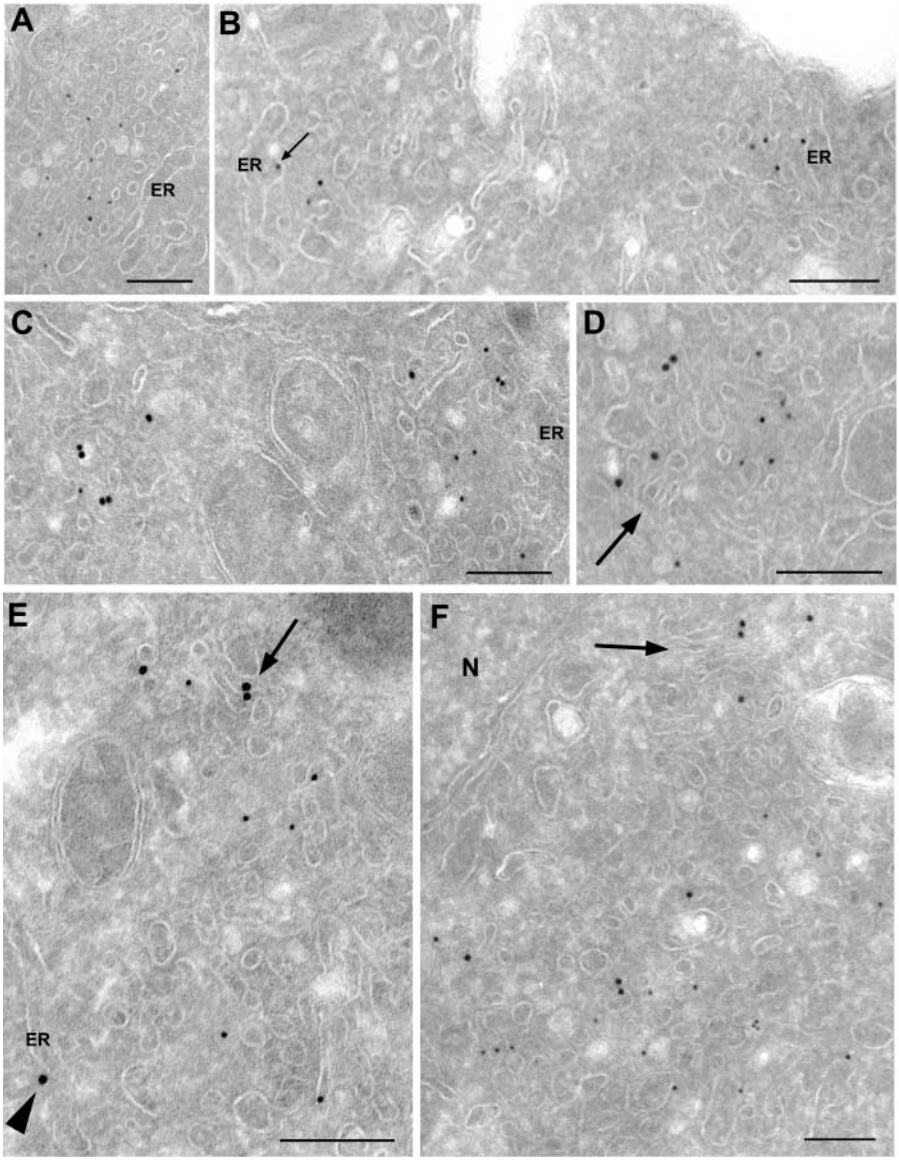

Figure 7. **Localization of dSec23p and d120kd in dp115-depleted cells.** S2 cells depleted of dp115 were processed for IEM and double labeled for dSec23p (10-nm gold) and d120kd (15-nm gold), as described in the legend of Fig. 5. (A–C) dSec23p-positive clusters. (C) d120kd-positive clusters. (D–F) Mixed clusters. A small arrow in B points to an ER bud labeled for dSec23p. Large arrows in D–F point to profiles reminiscent of Golgi cisternal remnants. Arrowhead in E points to a gold particle corresponding to d120kd associated with an ER cisterna. Note that in D–F, the labeling for dSec23p and d120kd marks differential regions of the same cluster. N, nucleus. Bars, 200 nm.

We verified that the induction and transport of Delta for as long as 2.5 h did not induce the rebuilding of Golgi stacks. In cells depleted of dp115 for 96 h, the percentage of cells with at least one Golgi stack was the same before and after Delta induction (18.0 ± 6.3 vs. 18.9 ± 1.2%, respectively).

We first induced Delta expression for 1 h followed by a 90-min chase as a way of measuring steady-state transport. In mock-treated and mock-depleted cells, a large majority of the staining was found at the plasma membrane (Fig. 9 A). Only 3.3 ± 2.5% of the cells exhibited exclusively intracellular (Fig. 9 B), with no plasma membrane, labeling.

The intensity of surface labeling at the plasma membrane varied considerably (Fig. 9 A). The estimation of the percentage of cells exhibiting the different labeling intensities allowed the calculation of the total intensity of the mock-treated cells (Fig. 9 D; Table I). This was set as 100% and was 90% inhibited by brefeldin A (Fig. 9, B and C; Table I), a known inhibitor of transport in the early exocytic pathway. Furthermore, an 89% transport inhibition was also obtained when cells were depleted of dSed5p, a protein largely documented for its role in intracellular transport (Fig. 9 C; Table I), suggesting that our transport assay was sufficiently sensitive to monitor an inhibition in transport and that Delta was a suitable marker for anterograde transport.

Depletion of dGM130 had only a negligible effect on the steady-state transport of Delta (Fig. 9 C; Table I). Surprisingly, depletion of dp115 reduced steady-state transport to a very small extent (~12%; Fig. 9 C; Table I).

The initial rate of transport in cells depleted for dp115, measured by inducing Delta expression for 25 min (minimal induction period to detect expression of the protein by Western blotting; unpublished data) and chasing for 45–90 min, was found to be reduced by 30.5 ± 3% when compared with mock-depleted cells (Fig. 9 D). The distribution of plasma membrane intensity was essentially the same in mock- and dp115-depleted cells where the exocytic pathway was largely modified (Fig. 9, compare E with F). This suggests that the large modifications to the morphology of the Golgi stacks and the tER organization caused by dp115 depletion did not make the cells incompetent for transport.

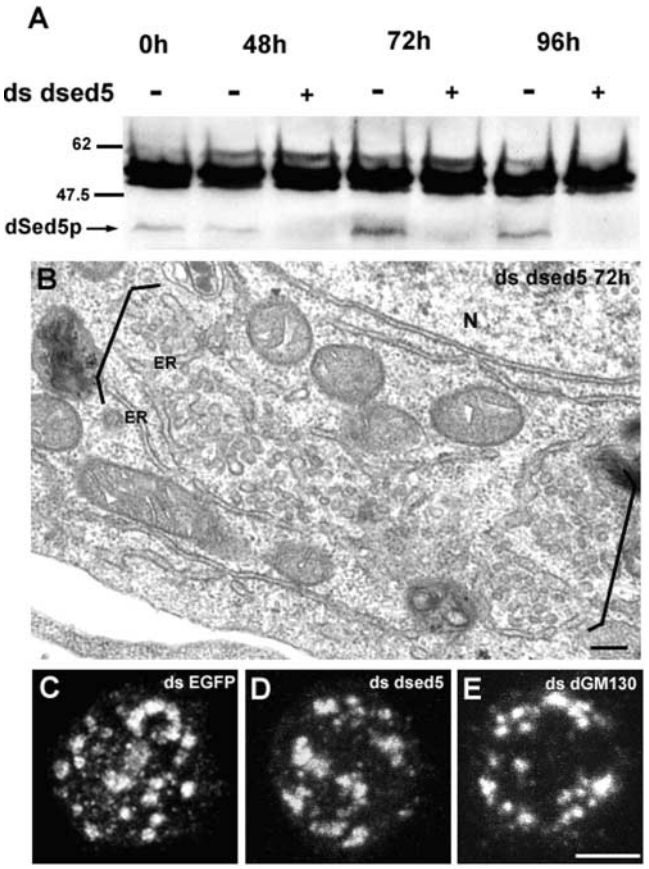

Figure 8. **Effect of dSed5p depletion on the Golgi stack morphology and tER organization.** (A) S2 cells were incubated with ds dsed5 up to 96 h. Extracts of mock- and dSed5p-depleted S2 cells were Western blotted using JSEE1 antibody. The 35-kD band corresponding to dSed5p is efficiently depleted (arrow). (B) The Golgi stack morphology in depleted cells was assessed by conventional EM. The cells exhibited no Golgi stacks, but extended areas completely vesiculated in >95% of the profiles examined. (C) The tER organization was monitored by immunofluorescence using the anti-Sec23p antibody, as described in the legend of Fig. 6, in control cells, (D) in cells depleted of dSed5p, and (E) in cells depleted of dGM130. N, nucleus. Bars: (B) 200 nm; (C–E) 5 μm.

Last, using a second S2 cell line where the expression of a secreted marker could be induced and monitored, we showed that the depletion of dp115 and dGM130 did not affect the secretion of this marker (unpublished data). This result strengthens the notion that the disorganization of the exocytic pathway does not lead to a significant decrease in transport efficiency.

Discussion

We have used *Drosophila* S2 cells to perform depletion of dp115 and dGM130 by RNA interference (RNAi). Despite small differences with mammalian cells, *Drosophila* cells are a novel, but adequate, biological system to investigate the issues related to membrane traffic and organelle structure.

dp115 localization

dp115 was localized on dSec23p-positive pleiomorphic membrane structures representing tERs, on the Golgi area, and on the ER cisternae. This distribution is slightly different from that in mammalian cells, where p115 has been localized in the cis Golgi, the Golgi stack, and the intermediate compartment (Nelson et al., 1998; Alvarez et al., 1999, 2001). Its localization on the tER sites was inferred only by the role it plays in priming COPII vesicles for fusion (Allan et al., 2000). This difference could be explained by the fact that the region between the ER and the Golgi stack comprised more layers in mammalian cells, including one positive for ERGIC53 that does not overlap with Sec13p (Hammond and Glick, 2000). In contrast, in S2 cells, the tER sites were found abutting the Golgi stack itself, as if the intermediate compartment was missing (a situation that seems similar to yeast where sec12/sec13 labeling seems to overlap with the Golgi apparatus; Rossanese et al., 1999; Bevis et al., 2002) or compressed into a single layer.

Golgi stacks are breaking down upon dp115 depletion

Depletion of dp115 in S2 cells led to the fragmentation of their Golgi stacks into clusters of vesicles and tubules. These clusters were labeled by a fraction of d120kd that, in mock-treated cells, preferentially marked the Golgi stacks. Some of them also seemed to contain remnants of Golgi cisternae. Furthermore, the Golgi stacks, in the small percentage of cells where they could still be observed, were 30% shorter than control. This suggests that upon dp115 depletion, Golgi stacks are fragmented into clusters retaining Golgi identity and function (see below). Similar results have been reported in mammalian cells that exhibited a fragmented

Table I. **Effect of depleting S2 cells of dp115, dGM130, and dSed5p on the efficiency of Delta intracellular transport to the plasma membrane**

Conditions	Efficiency of intracellular transport	
	Steady state (60 min/90 min)	Initial rate (25 min/45–90 min)
Mock treated	100%	100%
Mock depleted	100%	100%
dGM130 depleted	94.1 ± 4.5% (n = 2)	ND
dp115 depleted	87.9 ± 1.4% (n = 2)	69.5 ± 3%
Brefeldin A treated	10% (n = 1)	ND
dSed5p depleted	11 ± 1% (n = 3)	ND

Transport was measured after depletion of the various proteins for 96 h. The efficiency of transport (initial and steady state) in the mock-treated cells was set at 100%. The results of the steady-state transport efficiency obtained after the various depletions are expressed as a fraction of the "steady-state" efficiency of mock-treated cells. The results of the "initial rate" obtained after dp115 depletion are expressed as a fraction of the "initial" rate of the mock-treated cells. The results are expressed ± SD.

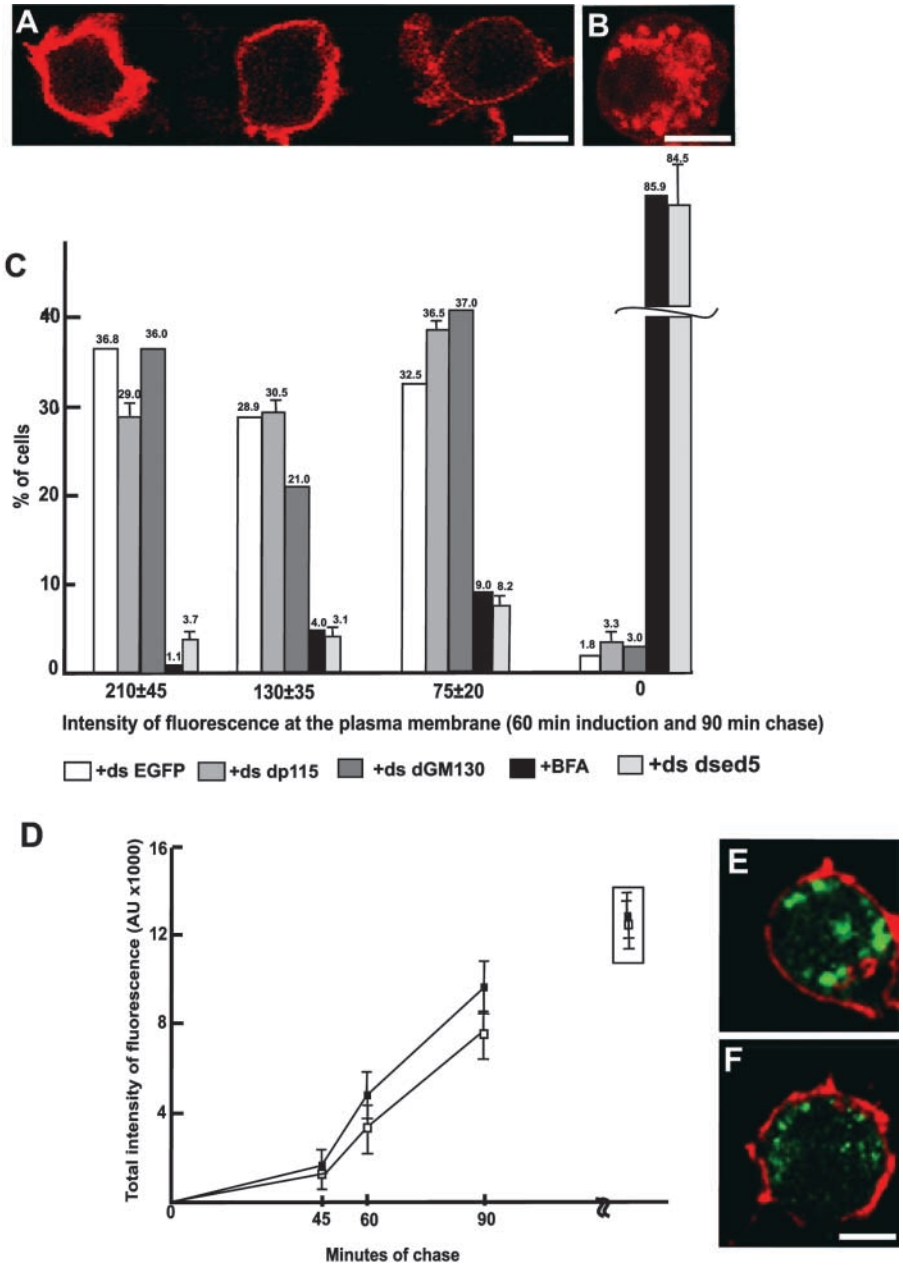

Figure 9. **Effect of protein depletion on Delta anterograde protein transport to the plasma membrane.** Delta S2 cells were incubated for 96 h with ds EGFP, ds dp115, ds dGM130, and ds dsed5, or treated with brefeldin A (BFA) (see Materials and methods). (A) Representation of the three categories of plasma membrane labeling intensity, after a 1-h induction of Delta followed by a 90-min chase. One confocal section is presented. (B) Example of exclusive intracellular Delta labeling. (C) Percentage of cells exhibiting the three different intensities of plasma membrane or exclusive intracellular labeling after Delta induction for 1 h followed by 90 min of chase. Results obtained with mock-depleted cells (+ds EGFP), cells depleted of dp115 (+ds dp115), dGM130 (+ds dGM130), or dSed5p (+ds dsed5), or cells treated with brefeldin A are expressed as the percentage of total number of cells examined. The error bars represent the SD. (D) Initial rate of transport in dp115-depleted (empty symbols) and mock-depleted (filled symbols) cells induced for 25 min followed by 45, 60, and 90 min of chase. The intensity of Delta labeling at the plasma membrane was estimated as described in the Materials and methods and plotted against the chase time. The boxed results represent the total intensity obtained after a 1-h induction and 90-min chase. Immunofluorescence picture of a mock-depleted cell (E) with a control dSec23p pattern (green) and Delta at the plasma membrane (red), and of a dp115-depleted cell (F) with a fragmented dSec23p pattern (green) and the same amount of Delta at the plasma membrane (red). One confocal section is presented. Bar, 5 μm.

Golgi ribbon upon depletion of p115 by antibody injection (Alvarez et al., 1999; Puthenveedu and Linstedt, 2001).

What could be the mechanism? Intracellular transport could be inhibited in dp115-depleted cells, and transport intermediates could accumulate and create the membrane clusters. In mammalian cells, p115 has been shown to have a role in intracellular transport by at least three mechanisms. First, it forms a complex with GM130 on the Golgi cisternae, and giantin on the COPI vesicles, that helps the vesicles to be in close proximity to their target membrane, enhancing docking efficiency and fusion (Nakamura et al., 1997; Sönnichsen et al., 1998). Second, p115 is recruited by activated rab1 onto the COPII budding vesicles, priming them for fusion (Allan et al., 2000). Third, p115 has recently been shown to catalytically promote the syntaxin5/Gos28 SNAREpin formation, suggesting a direct role in vesicle docking and fusion (Shorter et al., 2002). Given the significant homology between dp115 and its mammalian counterpart, dp115 could have an equivalent role in intracellular transport. However, we found that anterograde intracellular transport was largely unaffected (see below), suggesting that as a sole mechanism, the reduction of docking/fusion of ER-derived transport vesicles is unlikely to be sufficient to explain the observed Golgi breakdown.

Mammalian p115 has also been involved in the building and maintenance of the Golgi stacks, independent of its role in transport (Puthenveedu and Linstedt, 2001; Shorter and Warren, 2002). First, in vitro NSF-mediated rebuilding of Golgi cisternae was shown to require p115 (Rabouille et al., 1995) (though that could due to its role in SNARE pairing). p115 was also involved in the in vitro stacking of the p97-mediated Golgi cisternae (Shorter and Warren, 1999). Last, it has been identified as a binding partner of GM130 in the GM130/GRASP65 complex (Barr et al., 1998). This tripar-

tite complex is proposed to be involved in the stacking of Golgi cisternae (Barr et al., 1997; Linstedt, 1999).

dp115 could be involved in a similar complex. Our unpublished results show that dp115 and dGM130 interact genetically and could therefore form a complex, perhaps with dGRASP, the single homologue of GRASP65 and 55. If the stacking mechanism were impaired by the removal of dp115, this would affect the morphology of the Golgi area. However, we did not observe single cisternae, suggesting that dp115 might have an additional role in the maintenance of the cisternae themselves, maybe in preventing their fission into smaller fragments. Furthermore, we have shown that depletion of dGM130 does not affect Golgi stack architecture, in agreement with Puthenveedu and Linstedt (2001) and Vasile et al. (2003). That dGM130, and its mammalian counterpart, has a direct role in the structure of the Golgi stack remains to be shown.

Depletion of dp115 affects tER organization

The alteration in the tER organization that we demonstrated in S2 cells depleted of dp115 could contribute to the breakdown of the Golgi stack architecture (see Introduction; Rossanese et al., 1999; Ward et al., 2001). Instead of the focused organization observed in control cells, the tERs were scattered into a multitude of smaller sites in dp115-depleted S2 cells. The organization of the tER/Golgi stacks in our mock-treated cells was reminiscent of that in *Pichia pastoris* (see Fig. 6 B in Rossanese et al., 1999), whereas in dp115-depleted S2 cells, it resembles *S. cerevisiae* (see Fig. 5 in Rossanese et al., 1999). Given our results, a differential localization of Uso1p or a binding partner between *Pichia* and *S. cerevisiae* could perhaps explain the difference in the organization of their exocytic pathways.

dp115 could therefore only have a role in tER organization. If that were the case, the dispersion of the tER sites would precede the change in the Golgi stack. Despite intensive searching for such profiles, only a very small percentage of cells fit these criteria, and to the same extent as cells in which the Golgi stack organization was lost while still exhibiting a normal tER pattern. Of course, the effect of the tER disorganization on the Golgi stack morphology could be very rapid. Only video microscopy could lead to a definitive answer on that issue. Nevertheless, this result suggests that dp115 is involved in Golgi stack morphology independently of its role in tER organization.

We propose that in *Drosophila*, dp115 has a role in both tER and Golgi stack organization. dp115 could be involved in at least two different complexes, one in the tERs (with unknown partners; Nelson et al., 1998) and one in the Golgi stacks (with perhaps dGM130). These two complexes could either form part of a common matrix underlying both the tERs and the Golgi stacks, as is the case in *Pichia* (Mogelsvang et al., 2003). The fact that in cells depleted of dSed5p, the Golgi stacks are completely vesiculated while the tER organization is intact leads us to propose that there are two independent matrices that have dp115 as a common component. Furthermore, it has been proposed that tERs and Golgi stacks would operate as a positive feedback loop on each other's organization by exchanging membrane and molecules (Hammond and Glick, 2000). dp115 could be an important part of this exchange program.

The dispersion of the tERs could also contribute to Golgi stack breakdown, by allowing the dispersion of budded vesicles that would not participate in the homeostasis/building of Golgi stacked cisternae. Whether Golgi stacks can form in cells comprising dispersed tER sites remains to be shown.

Intracellular transport is only marginally reduced in cells depleted of dp115

The anterograde protein transport in cells depleted of dp115, in which both the Golgi stacks and the tER sites are disorganized, was only marginally affected, shown by two independent assays. Supporting this result, cell proliferation was not affected in dp115 depletion (unpublished data), suggesting that, as for the protein markers used in our experiments, endogenous proteins were likely to be transported as efficiently in depleted cells.

This result is different from those recently published where the injection of a p115 antibody in mammalian cells disrupts the Golgi ribbon and strongly inhibits the ER to Golgi transport (Alvarez et al., 1999, 2001). Furthermore, the injection of a GM130 cDNA encoding a form of GM130 lacking its p115 binding domain also inhibited anterograde transport by 65% (Seemann et al., 2000b). The same holds true for the depletion of dGM130 that did not lead to an inhibition of intracellular transport in our assay, contrary to mammalian cell studies (Alvarez et al., 2001). These differences could be explained by the methodology used for the depletion or perhaps suggest that dp115 and dGM130, unlike their mammalian counterparts, do not have a role in intracellular transport.

However, we find it quite surprising. A strong structural similarity between dp115 and mammalian p115 exists. The SNARE motif identified in mammalian SNARES (Weimbs et al., 1997) is also present in dp115 (amino acids 664–729; unpublished data), suggesting that like its mammalian counterpart, it could also catalyze SNAREpin assembly between dSed5p and dGos28, which also contains a SNARE motif (Weimbs et al., 1997; unpublished data). Given that the role of p115 is catalytic at least in vitro, a trace amount of dp115 could serve its function in transport. Although we show that the dp115 mRNA and protein were successfully depleted, we think that trace amounts of protein remain, a limitation of RNAi techniques. Therefore, we instead conclude that the role of dp115 in contributing to the Golgi stack structure and tER organization can be separated from its role in intracellular transport.

We show here, as is the case in yeast, that *Drosophila* intracellular transport can be sustained by more than one type of exocytic pathway, including dispersed tERs and fragmented Golgi stacks. Clearly, smaller and multiple tER sites and Golgi clusters of vesicles and tubules can efficiently perform this transport function. This could explain the existence of developmental stages in *Drosophila* in which cells do not exhibit Golgi stacks but exhibit clusters of vesicles and tubules instead, as in the case of the third instar larval imaginal discs (Kondylis et al., 2001). Perhaps this flexibility is not offered to mammalian cells, with their unique organization of the

Golgi complex involving the formation of the single copy Golgi ribbon.

Thus, what is the role of Golgi stacks if efficient anterograde transport can take place in their absence? Golgi stacks (but not Golgi clusters) could have a role in retrograde transport, in the proper and complete maturation of protein-born O- and N-linked oligosaccharide moieties and the addition of sorting signals. This is for further investigation.

Materials and methods

Double-stranded RNA

dp115 cDNA was cloned by screening an embryonic cDNA library with a DNA probe made using the EST LD41079. The dp115 cDNA (1P2C1) was used to PCR a 682-bp fragment with flanking T7 RNA polymerase binding sites using the 5′ primer TAATACGACTCACTATAGGGAGA(T7)-acccagaatagac and the 3′ primer T7-tcaaaaaggcggtca. The 774-bp T7-dGM130 template was obtained by PCR from the clone p5.6KK (provided by Terry Orr-Weaver, Whitehead Institute, Cambridge, MA) containing the MeiS332 gene (Kerrebrock et al., 1995) and the coding sequence of dGM130 using the 5′ primer T7-cgccagcaacaacaa and the 3′ primer T7-tgctccttgtcctgcgtt. The 635-bp T7/T3-EGFP template (gift from Thomas Vaccari, European Molecular Biology Laboratory [EMBL], Heidelberg, Germany) was obtained using the 5′ primer T7-taaacggccacaagttcag and the 3′ primer AATTAACCCTCACTAAAGGGAGA(T3)-gtgatcgcgcttctcgttg. Finally, the 733-bp T7/T3-dsed5 template (gift from Thomas Vaccari) was obtained using the 5′ primer T7-gcttatttgatgacagac and the 3′ primer T3-aatatgagaacgccgaag.

The various T7 and T3 templates were purified from the agarose gel using the GFX PCR DNA and gel band purification kit (Amersham Biosciences). The purified products were used as templates for dsRNA synthesis using the MEGASCRIPT T7 and T3 transcription kit (Ambion) according to manufacturer's standard protocol.

Cell cultures and dsRNA interference

S2 cells were grown in Schneider's insect medium supplemented with 10% heat-inactivated and insect-tested FBS at 27°C in a humidified atmosphere. Delta-WTNdeMYC S2 cells (Delta S2 cells) were a gift from Kris Klueg (Indiana University, Bloomington, IN). Delta S2 is a stable cell line expressing the full-length Delta protein at the plasma membrane upon induction with 1 mM $CuSO_4$ (Klueg et al., 1998). The Delta S2 cell line was cultured in the presence of 2×10^{-6} M methotrexate (ICN Biomedicals).

RNAi was performed in both cell lines as described in Clemens et al. (2000). 1,000,000 cells/well in DES serum-free medium (Invitrogen) were incubated with 20–30 μg of the various dsRNAs for 30 min at room temperature followed by the addition of 2 ml of Schneider's medium containing FBS and methotrexate in the case of Delta S2 cells. Mock-treated and mock-depleted cells were treated in the same way except that no dsRNA or ds EGFP was added, respectively. They were considered as controls.

Antibodies

dGM130 was detected using a rabbit polyclonal antibody directed against the first 73 amino acids of human GM130 (MLO7; gift from Martin Lowe), as described in Kondylis et al. (2001). dp115 was detected with a rabbit polyclonal antibody raised against the peptide (G)CSKLAEVSRHEAYSRA, which corresponds to amino acids 584–599 from dp115 (Biosynthesis), and purified against the peptide coupled to EAH–Sepharose 4B (Amersham Biosciences) activated by Sulfo-MBS cross-linker (Pierce Chemical Co.) (dp115/584). dSec23p was detected using a rabbit polyclonal antibody raised against the first 18 amino acids of mammalian Sec23p (Affinity BioReagents, Inc.), sharing 90% identity with the equivalent peptide of dSec23p. d120kd was detected with a mouse monoclonal antibody recognizing a 120-kD integral Golgi membrane protein in *Drosophila* (Calbiochem). dSed5p was detected using a rabbit polyclonal antibody raised against mammalian syntaxin 5 (JSEE1; gift from Martin Lowe). Delta was detected using C594.9B, a mouse monoclonal antibody raised against its extracellular domain (DSHB; University of Iowa).

Western blotting

The same number of cells (typically from 1,000,000 to 2,500,000) incubated with or without dsRNA for each time point was harvested, spun, and homogenized in 25 μl buffer containing 20 mM Tris-HCl, 1 mM EDTA, 10 mM $MgCl_2$, 10 mM KCl, 10 mM NaCl, 1 mM DTT, 0.23 M sucrose, and 1% Triton X-100 and protease inhibitors using a motorized pestle. In the case of dp115 detection, cells were homogenized in the absence of Triton and with protease inhibitor cocktail (Roche). The SDS sample buffer was added to a 1× final concentration. The membrane fraction was prepared as follows. 10,000,000 cells were cracked using a 30-gauge needle in the homogenization buffer and protease inhibitors. After a short spin to remove cell debris and nuclei, the extract was spun for 1 h at 100,000 *g* to separate the cytosol from the membrane. The membrane pellet was recovered in 40 μl 1× SDS sample buffer. Total extract of one third instar *Drosophila* larvae and 20 embryos was prepared by homogenization using a motorized pestle in 40 μl of the homogenization buffer. The total extract, the membrane pellets, and 4% of the cytosolic fraction were fractionated on a 10% acrylamide gel and detected by Western blots using MLO7, the affinity-purified dp115 antibody, JSEE1, Sec23p antibody, and d120kd antibody, followed by the appropriate secondary antibody coupled to HRP (Vector Laboratories). ECL (Amersham Biosciences) was used for the visualization of the bands.

RT-PCR

Total RNA was extracted from 1,000,000 S2 cells using the Purescript RNA isolation kit (Flowgen). The RT reactions were performed with the Superscript II reverse transcriptase kit (Invitrogen) according to the company's protocol and using 1 μg of total RNA.

The RT products were diluted 1/20 and were used in the PCR reaction with the 5′ primer agttcctgaagagtggcatcaa and the 3′ primer gctatctggacgaatacgat for dp115, leading to a 414-bp fragment (corresponding to the 5′ end of the dp115 gene), and the 5′ primer gtggaaaaggtggcaaagtgaa and 3′ primer atgctggtgacaacaagaa for histone 2A (H2A), leading to a 213-bp fragment. The four primers were added in the same reaction.

Conventional EM

Cells were fixed for 2 h in 1% glutaraldehyde in 0.2 M phosphate buffer (pH 7.4) and processed for conventional EM as described in Kondylis et al. (2001).

IEM

Control or depleted S2 cells (96 h) were fixed in 2% PFA and 0.2% glutaraldehyde (GA) (2 h at room temperature) or 4% PFA alone (overnight at 4°C) in 0.2 M phosphate buffer, pH 7.4. Oregon R third instar salivary glands were dissected as described in Dunne et al. (2002), fixed in 2% PFA and 0.2% GA overnight at 4°C in the same buffer as described above. Both cells and tissues were processed for IEM as described previously (Liou et al., 1996). In brief, immunolabeling was performed using the described primary antibodies followed directly by protein A conjugated to gold particles (protein A gold), in the case of rabbit antibodies. In the case of a mouse antibody, a bridging step of rabbit anti–mouse IgG was used followed by protein A gold.

Stereology

The Golgi area was defined by the Golgi stacked cisternae and immediate surrounding vesicles and tubules. When Golgi stacks were not observed, the Golgi area was defined as the clusters of vesicles and tubules occupying the position where Golgi stacks are normally found, nested near an ER cisterna in 80% of the cases. Vesicles, tubules, cisternae, and Golgi stacks are defined in Kondylis et al. (2001).

The percentage of cell profiles exhibiting at least one Golgi stack was estimated by randomly analyzing under the transmission electron microscope >100 cell profiles taken from at least two grids and two different experiments. The percentage of membrane in cisternae, tubules, or vesicles per Golgi area and the surface density of the Golgi area and total cisternae were estimated as described in Kondylis et al. (2001). The linear density was determined by the intersection method.

Delta transport assay

Delta S2 cells plated on glass coverslips were treated with dsRNA for given periods of time to deplete the protein of interest, typically 96 h. 1 mM $CuSO_4$ was added to the culture media to induce the production of Delta. After 25 min at 27°C, the media were replaced with new Schneider's media without $CuSO_4$, and the transport of Delta to the plasma membrane was chased for up to 90 min (initial transport of Delta). We also induced the synthesis of Delta for 60 min followed by a chase of 90 min (steady-state transport of Delta). Delta transport was also measured in cells treated with 50 μM brefeldin A for 30 min at 37°C, followed by induction with $CuSO_4$ and chase at 27°C in the presence of brefeldin A.

Indirect immunofluorescence

S2 cells were fixed for 20 min in 3% PFA in PBS at room temperature and processed for immunofluorescence (Rabouille et al., 1999) after permeabi-

lization with Triton. dSec23p and d120kd were detected using the antibodies described above followed by anti–rabbit IgG coupled to Alexa 488 and anti–mouse IgG coupled to Alexa 568 (Molecular Probes), respectively. Delta S2 cells were processed in the same way. Delta protein was labeled using C594.9B antibody followed by an anti–mouse IgG coupled to Texas red (Vector Laboratories). Cells were viewed under a Leica confocal microscope. A series of 30 sections through the cells were collected, and projections were reconstituted and presented unless otherwise stated.

Quantitation of Delta transport to the plasma membrane

Equatorial sections of random cells from each sample were captured with the Leica confocal microscope using a 63× water lens. Control cells were analyzed first so that the highest intensity of labeling was within the dynamic range of the laser. This set up was maintained for the analysis of the depleted cells.

The surface labeling intensity was estimated using the Leica software, which is able to measure and display the intensity of labeling along a line that is drawn perpendicular to the plasma membrane. In this way, the intensity peak as well as the thickness of the labeled plasma membrane were estimated. Typically, cells induced for 1 h followed by a 90-min chase displayed a large range of intensity and were ranked into three categories: 210 ± 45, 130 ± 35, and 75 ± 20 intensity units per plasma membrane cross section. The intensity was essentially constant around the perimeter of the cell.

About 300–500 cells for each condition were quantitated, and the results were expressed as a percentage of cells exhibiting each of the three categories of intensity. The total intensity in each condition was calculated using an arithmetic sum $\Sigma I \times N \times p$, where I is the intensity, N is the percentage of cells exhibiting intensity I, and p is the perimeter length of the plasma membrane. The perimeter length was not taken into account because both control and depleted cells had similar mean diameters and their almost spherical shape did not change. The total intensity was considered as 100% for the control cells, while the efficiency of intracellular transport in treated/depleted cells was expressed as a ratio of their total intensity versus that of the control cells. The same procedure was reproduced for cells induced for 25 min and chased for 45, 60, and 90 min. Again the intensity of labeling at the plasma membrane was measured as described above and ranked into three categories that vary slightly with the time of chase. The total intensity was calculated as an absolute value.

Online supplemental material

The supplemental material (Figs. S1–S4) is available at http://www.jcb.org/cgi/content/full/jcb.200301136/DC1. A concise description of the data presented in each supplementary figure is introduced upon citation in the text. Details on the experimental procedure and further comments on data reported can be found in the legends.

We wish to thank Martin Lowe for his gift of antibodies, Kris Klueg for her gift of the Delta cell line, Terry Orr-Weaver for the cDNA clone containing dGM130 sequence, Jonathan Dunne for critically reading and editing the manuscript, Elly van Donselaar for her help with IEM, Dagmar Zeuschner for her help with the affinity purification of the dp115 antiserum, and Thomas Vaccari and Anne Ephrussi (EMBL) for their gift of EGFP and dsed5 primers. We acknowledge the use of Flybase, the Berkeley *Drosophila* genome project, and Gadfly.

V. Kondylis was supported by the Darwin Trust of Edinburgh. C. Rabouille was supported by a fellowship from the Medical Research Council (UK) and by the Department of Cell Biology, Utrecht.

Submitted: 30 January 2003
Revised: 15 May 2003
Accepted: 3 June 2003

References

Allan, B.B., B.D. Moyer, and W.E. Balch. 2000. Rab1 recruitment of p115 into a cis-SNARE complex: programming budding COPII vesicles for fusion. *Science.* 289:444–448.

Alvarez, C., H. Fujita, A. Hubbard, and E. Sztul. 1999. ER to Golgi transport: requirement for p115 at a pre-Golgi VTC stage. *J. Cell Biol.* 147:1205–1222.

Alvarez, C., R. Garcia-Mata, H.P. Hauri, and E. Sztul. 2001. The p115-interactive proteins GM130 and giantin participate in endoplasmic reticulum-Golgi traffic. *J. Biol. Chem.* 276:2693–2700.

Banfield, D.K., M.J. Lewis, C. Rabouille, G. Warren, and H.R. Pelham. 1994. Localization of Sed5, a putative vesicle targeting molecule, to the cis-Golgi network involves both its transmembrane and cytoplasmic domains. *J. Cell Biol.* 127:357–371.

Bannykh, S.I., T. Rowe, and W.E. Balch. 1996. The organization of endoplasmic reticulum export complexes. *J. Cell Biol.* 135:19–35.

Barlowe, C., L. Orci, T. Yeung, M. Hosobuchi, S. Hamamoto, N. Salama, M.F. Rexach, M. Ravazzola, M. Amherdt, and R. Schekman. 1994. COPII: a membrane coat formed by Sec proteins that drive vesicle budding from the endoplasmic reticulum. *Cell.* 77:895–907.

Barr, F.A., M. Puype, J. Vandekerckhove, and G. Warren. 1997. GRASP65, a protein involved in the stacking of Golgi cisternae. *Cell.* 91:253–262.

Barr, F.A., N. Nakamura, and G. Warren. 1998. Mapping the interaction between GRASP65 and GM130, components of a protein complex involved in the stacking of Golgi cisternae. *EMBO J.* 17:3258–3268.

Bevis, B.J., A.T. Hammond, C.A. Reinke, and B.S. Glick. 2002. De novo formation of transitional ER sites and Golgi structures in *Pichia pastoris. Nat. Cell Biol.* 4:750–756.

Clemens, J.C., C.A. Worby, N. Simonson-Leff, M. Muda, T. Maehama, B.A. Hemmings, and J.E. Dixon. 2000. Use of double-stranded RNA interference in *Drosophila* cell lines to dissect signal transduction pathways. *Proc. Natl. Acad. Sci. USA.* 97:6499–6503.

Dirac-Svejstrup, A.B., J. Shorter, M.G. Waters, and G. Warren. 2000. Phosphorylation of the vesicle-tethering protein p115 by a casein kinase II–like enzyme is required for Golgi reassembly from isolated mitotic fragments. *J. Cell Biol.* 150:475–487.

Dunne, J.C., V. Kondylis, and C. Rabouille. 2002. Ecdysone triggers the expression of Golgi genes in *Drosophila* imaginal discs via broad-complex. *Dev. Biol.* 245:172–186.

Hammond, A.T., and B.S. Glick. 2000. Dynamics of transitional endoplasmic reticulum sites in vertebrate cells. *Mol. Biol. Cell.* 11:3013–3030.

Glick, B.S. 2002. Can the Golgi form de novo? *Nat. Rev. Mol. Cell Biol.* 3:615–619.

Kerrebrock, A.W., D.P. Moore, J.S. Wu, and T.L. Orr-Weaver. 1995. Mei-S332, a *Drosophila* protein required for sister-chromatid cohesion, can localize to meiotic centromere regions. *Cell.* 83:247–256.

Klueg, K.M., T.R. Parody, and M.A. Muskavitch. 1998. Complex proteolytic processing acts on Delta, a transmembrane ligand for Notch, during *Drosophila* development. *Mol. Biol. Cell.* 9:1709–1723.

Kondylis, V., S.E. Goulding, J.C. Dunne, and C. Rabouille. 2001. The biogenesis of the Golgi stacks in the imaginal discs of *Drosophila melanogaster. Mol. Biol. Cell.* 12:2308–2327.

Linstedt, A.D. 1999. Stacking the cisternae. *Curr. Biol.* 9:R893–R896.

Liou, W., H.J. Geuze, and J.W. Slot. 1996. Improving structural integrity of cryosections for immunogold labeling. *Histochem. Cell Biol.* 106:41–58.

Mogelsvang, S., N. Gomez-Ospina, J. Soderholm, B.S. Glick, and L.A. Staehelin. 2003. Tomographic evidence for continuous turnover of Golgi cisternae in *Pichia pastoris. Mol. Biol. Cell.* 14:2277–2291.

Morsomme, P., and H. Riezman. 2002. The Rab GTPase Ypt1p and tethering factors couple protein sorting at the ER to vesicle targeting to the Golgi apparatus. *Dev. Cell.* 2:307–317.

Munro, S., and M. Freeman. 2000. The Notch signalling regulator fringe acts in the Golgi apparatus and requires the glycosyltransferase signature motif DXD. *Curr. Biol.* 10:813–820.

Nakamura, N., M. Lowe, T.P. Levine, C. Rabouille, and G. Warren. 1997. The vesicle docking protein p115 binds GM130, a cis-Golgi matrix protein, in a mitotically regulated manner. *Cell.* 89:445–455.

Nelson, D.S., C. Alvarez, Y.S. Gao, R. Garcia-Mata, E. Fialkowski, and E. Sztul. 1998. The membrane transport factor TAP/p115 cycles between the Golgi and earlier secretory compartments and contains distinct domains required for its localization and function. *J. Cell Biol.* 143:319–331.

Orci, L., M. Ravazzola, P. Meda, C. Holcomb, H.P. Moore, L. Hicke, and R. Schekman. 1991. Mammalian Sec23p homologue is restricted to the endoplasmic reticulum transitional cytoplasm. *Proc. Natl. Acad. Sci. USA.* 88:8611–8615.

Panin, V.M., L. Shao, L. Lei, D.J. Moloney, K.D. Irvine, and R.S. Haltiwanger. 2002. Notch ligands are substrates for protein O-fucosyltransferase-1 and Fringe. *J. Biol. Chem.* 277:29945–29952.

Preuss, D., J. Mulholland, A. Franzusoff, N. Segev, and D. Botstein. 1992. Characterization of the *Saccharomyces* Golgi complex through the cell cycle by immunoelectron microscopy. *Mol. Biol. Cell.* 3:789–803.

Puthenveedu, M.A., and A.D. Linstedt. 2001. Evidence that Golgi structure depends on a p115 activity that is independent of the vesicle tether compo-

nents Giantin and GM130. *J. Cell Biol.* 155:227–238.

Rabouille, C., T.P. Levine, J.M. Peters, and G. Warren. 1995. An NSF-like ATPase, p97, and NSF mediate cisternal regrowth from mitotic Golgi fragments. *Cell.* 82:905–914.

Rabouille, C., D.A. Kuntz, A. Lockyer, R. Watson, T. Signorelli, D.R. Rose, M. Van den Heuvel, and D.B. Roberts. 1999. The *Drosophila GMII* gene encodes Golgi α-mannosidase II. *J. Cell Sci.* 112:3319–3330.

Rossanese, O.W., J. Soderholm, B.J. Bevis, I.B. Sears, J. O'Connor, E.K. Williamson, and B.S. Glick. 1999. Golgi structure correlates with transitional endoplasmic reticulum organization in *Pichia pastoris* and *Saccharomyces cerevisiae*. *J. Cell Biol.* 145:69–81.

Sapperstein, S.K., D.M. Walter, A.R. Grosvenor, J.E. Heuser, and M.G. Waters. 1995. p115 is a general vesicular transport factor related to the yeast endoplasmic reticulum to Golgi transport factor uso1p. *Proc. Natl. Acad. Sci. USA.* 92:522–526.

Seemann, J., E. Jokitalo, M. Pypaert, and G. Warren. 2000a. Matrix proteins can generate the higher order architecture of the Golgi apparatus. *Nature.* 407: 1022–1026.

Seemann, J., E. Jokitalo, and G. Warren. 2000b. The role of the tethering proteins p115 and GM130 in transport through the Golgi apparatus in vivo. *Mol. Biol. Cell.* 11:635–645.

Shorter, J., and G. Warren. 1999. A role for the vesicle tethering protein, p115, in the post-mitotic stacking of reassembling Golgi cisternae in a cell-free system. *J. Cell Biol.* 146:57–70.

Shorter, J., and G. Warren. 2002. Golgi architecture and inheritance. *Annu. Rev. Cell Dev. Biol.* 18:379–420.

Shorter, J., M.B. Beard, J. Seemann, A.B. Dirac-Svejstrup, and G. Warren. 2002. Sequential tethering of Golgins and catalysis of SNAREpin assembly by the vesicle-tethering protein p115. *J. Cell Biol.* 157:45–62.

Sönnichsen, B., M. Lowe, T. Levine, E. Jämsa, A.B. Dirac-Svejstrup, and G. Warren. 1998. A role for giantin in docking COPI vesicles to Golgi membranes. *J. Cell Biol.* 140:1013–1021.

Stanley, H., J. Botas, and V. Malhotra. 1997. The mechanism of Golgi segregation during mitosis is cell type-specific. *Proc. Natl. Acad. Sci. USA.* 94:14467–14470.

Vasile, E., T. Perez, N. Nakamura, and M. Krieger. 2003. Structural integrity of the Golgi is temperature sensitive in conditional-lethal mutants with no detectable GM130. *Traffic.* 4:254–272.

Ward, T.H., R.S. Polishchuk, S. Caplan, K. Hirschberg, and J. Lippincott-Schwartz. 2001. Maintenance of Golgi structure and function depends on the integrity of the ER export. *J. Cell Biol.* 155:557–570.

Weimbs, T., S.H. Low, S.J. Chapin, K.E. Mostov, P. Bucher, and K. Hofmann. 1997. A conserved domain is present in different families of vesicular fusion proteins: a new superfamily. *Proc. Natl. Acad. Sci. USA.* 94:3046–3051.